PCCP

HD $J \neq 0$ bound state resonances above the Cu (001) surface: The effects of physisorption anisotropy and the observation of anomalous Debye–Waller behavior at resonance conditions

L. V. Goncharova,[a] B. J. Hinch,[a] A. Hellman,[b] M. Hassel[b] and M. Persson[b]

[a] *Department of Chemistry and Laboratory of Surface Modification, Rutgers University, 610 Taylor Road, Piscataway, NJ 08854*
[b] *Department of Applied Physics, Chalmers University of Technology and Göteborg University, S-412 96 Göteborg, Sweden*

Received 12th September 2002, Accepted 3rd January 2003
First published as an Advance Article on the web 24th January 2003

The laterally averaged HD–Cu (001) physisorption potential has been investigated in studies of rotationally mediated selective adsorption resonances. To first approximation the results are consistent with those from other isotope systems, *i.e.*, H_2 and D_2 above Cu (001). The additional effects of the translational to rotational coupling, of HD, on the resonance levels have also been investigated theoretically. The measured resonance energies are in best agreement with calculations of the $J = 1$, 2 and $m_J = 0$ states. The zero temperature resonance energy widths are considerably broader than the experimental resolution function. In addition, surface temperature variations are shown to have two prominent effects: first on the strength of the resonant structure and, second, on resonance line widths. We attribute these effects to substrate phonon coupling with the resonantly bound HD species. Also, weak shifts of all resonance levels observed on hydrogen chemisorption are accompanied by further increases of resonance line widths.

Introduction

Molecular hydrogen above a Cu (001) surface represents a system whose interactions have been the focus of many theoretical and experimental studies.[1–6] Hydrogen weakly physisorbs on copper surfaces and dissociative chemisorption appears strongly activated.[7] At surface temperatures above ~10 K the clearest manifestations of the molecular physisorption interaction potential are in the effects of the short-lived bound state resonances.[8] In this paper, measurements of the rotationally-elastic, specularly-scattered, HD peak intensity are used to evaluate those resonance conditions for the molecular HD bound states above the Cu (001) surface. Close comparison will be made with results, from other workers,[9–12] of the D_2 and H_2 bound states on the same system.

Two distinct mechanisms have been widely accepted for the predominant coupling of an incident molecule into a bound state: diffractionally mediated selective adsorption (DMSA) and rotationally mediated selective adsorption (RMSA). Both mechanisms are approximately described by the resonant condition equation:

$$\varepsilon_\nu = \frac{\hbar^2}{2m}\left[\vec{k}_i^2 - \left(\vec{K}_{\|i} + \vec{G}\right)^2\right] + \Delta E_{\mathrm{rot}} \qquad (1)$$

where ε_ν is the (negative) energy of the νth stationary state in the laterally averaged potential well, and ΔE_{rot} is the change in rotational energy of the molecule on entering the νth bound state. (Strictly, the ε_ν are also weak functions of $K_{\|i}$, as the interaction potential can also show weak lateral variations.) For flat surfaces, such as fcc (111) or (100) metal faces, the DMSA mechanism is quite inefficient as the surface corrugation is low, and there is poor coupling of the molecule to momentum transfers with non zero surface reciprocal lattice vectors, G. For the majority of this paper the Cu (001) surface is considered to be essentially flat and we are concerned only with the RMSA process. The $(\hbar^2/2m)[\vec{k}_i^2 - (\vec{K}_{\|i} + \vec{G})^2]$ term of eqn. (1) then can be simplified to $(\hbar^2/2m)k_i^2\cos^2\Theta_i$, *i.e.*, for the $G = (0,0)$ condition alone. The last expression shows that the resonance condition depends not solely on the incident wavevector k_i, but rather on its "perpendicular" projection. While bearing in mind that energy is a scalar quantity, a "perpendicular energy" can be introduced:

$$E_{\mathrm{perp}} = E_i \cos^2\Theta_i \qquad (2)$$

and eqn. (1) reduces to the simple expression;

$$E_\nu = E_{\mathrm{perp}} + \Delta E_{\mathrm{rot}} \qquad (3)$$

We need to consider the consequences of surface-parallel momentum transfers to explain only one feature of the data; *i.e.*, evidence of a combined rotationally-inelastic and diffraction event (that is discussed later in this paper). Studies of HD diffraction from the Cu (001) surface are presented elsewhere.[13]

The weak physisorption potential for hydrogen interaction with the copper surface is thus well characterized by the laterally averaged form:

$$V(z,\theta) = V^\circ(z) + \sum_l V^l(z) P_l(\cos\theta) \qquad (4)$$

where z is the distance between the molecular electronic center and the surface, θ is the coordinate that specifies the molecular polar orientation, $V^\circ(z)$ is the isotropic component of the interaction potential, and the second set of terms accounts for any orientational anisotropy. All $V^l(z)$ terms, with l odd, necessarily equal zero. Theory[10] and experiment[1] indicate that the electronic structure of H_2, D_2 or HD is close to spherical, *i.e.*, $V^2(z)$ is weak but finite in the attractive region of the interaction (large z). The anisotropy of the interaction potential,

above Cu (001), was deduced from the n-H_2 level splitting of DMSA resonances[10] The preferred molecular orientation is perpendicular to the surface.

As $V^2(z)$ is small, the rotational excitation cross sections for the homonuclear isotopes are relatively small. In contrast, the heteronuclear molecule can undergo a facile rotational excitation upon surface scattering. The molecular center of mass of the HD molecule is displaced (by a distance $a = 0.164$ Å) from the electronic/interaction-potential center. If z' signifies the distance between the center of mass and the surface, for HD $z' = z - a\cos\theta$. The potential experienced, with a fixed center of mass, depends strongly on the orientation of the molecule. The interaction potential can now be expressed in terms of z':[5,14]

$$V_{\mathrm{HD}}(z',\theta) = V_{\mathrm{HD}}{}^{\circ}(z') + \sum_{l} V_{\mathrm{HD}}{}^{l}(z')P_l(\cos\theta) \qquad (5)$$

$V_{\mathrm{HD}}{}^{l}(z')$ terms, with l odd, are no longer necessarily zero. To a first approximation:

$$V_{\mathrm{HD}}{}^{l}(z') = -\alpha\frac{\mathrm{d}V^{\circ}(z')}{\mathrm{d}z'} \qquad (6)$$

with $\alpha = a$. θ is the angle between the HD molecular axis and the surface normal, θ being zero when the D atom is closest to the surface. The leading $V_{\mathrm{HD}}{}^{l}(z')$ term in eqn. (5) gives rise to the facile rotational excitation of HD and rotational to translational coupling.

As $V^{\circ}(z)$ has been so well characterized for H_2 and D_2 (ref. 2), can this potential be used to reproduce the energies of the HD bound state resonances, $E_{\nu}(\nu,J,m_J)$, where J and m_J refer to the rotational quantum numbers of the HD molecule? The explicit effects of the translational to rotational coupling of the heteronuclear isotope will be investigated in multidimensional calculations of the resonance structure. We compare also the calculational predictions for the resonance levels with experimentally determined values. In addition, studies of the influence of surface temperature variation on the bound state resonance features are presented. Finally, discernible shifts in HD bound state levels are induced by dissociative chemisorption of H_2. An approximate potential well depth of 32.5 meV is found for HD above a H-saturated Cu (001) surface.

I. Experimental

Briefly, a rotationally cold ($J = 0$) HD molecular beam was produced by catalytic conversion of H_2 and D_2, and seeding in helium. The beam underwent supersonic expansion, was scattered from the crystalline surface and was detected by electron impact ionization and mass selection (mass 3) in a RF quadrupole mass spectrometer. The back-scattered intensity was monitored at the specular reflectivity condition, with a total scattering angle of 99°, ($\Theta_i = 49.5°$.) A velocity resolution, $\Delta v/v$, was determined by time-of-flight (TOF) measurements to be typically of order 2.5%. The incident energy, E_i, of the nearly monoenergetic HD beam was varied by linear control of the nozzle temperature (40 K $< T_{\mathrm{noz}} <$ 330 K). Each scan presented here represents one TOF measurement showing the accumulation of all measured HD molecules during the course of that scan. (A similar methodology has been used for HD studies above other surfaces[8]) The long-range scans (from $E_{\mathrm{perp}} = 5$ meV to 25 meV, *i.e.*, for $E_i \sim 12$ meV to 60 meV) were of approximately 4 h duration. A full description of the apparatus and other experimental details of the HD beam are presented elsewhere.[13]

A Cu (001) sample was held under ultra high vacuum conditions, with a base pressure $\sim 1 \times 10^{-10}$ mbar. (The latter figure excludes added He, H_2, D_2 and HD partial pressures from the beam source). The sample was prepared by repeated cycles of sputtering at room temperature (30 min, Ne^+, 600 eV, 5 μA cm^{-2}) and heating to 675 K for 10 min, followed by a final anneal to 900 K. When required, dissociative adsorption of hydrogen was achieved by backfilling the chamber with H_2 ($p = 10^{-6}$ mbar) in the presence of a white hot tungsten filament, with the surface temperature $T_x = 170$ K. Hydrogen exposures are characterized by monitoring specular helium atom reflectivities. A constant hydrogen exposure was reproduced by using to a helium signal drop of ~2.5 orders of magnitude. Splitting of the ($\pm 1/2$ 0) and (0 $\pm 1/2$) diffraction peaks were observed in the out-of-plane angular distribution scans. These peaks are characteristic of the p(2 × 1) hydrogen structure with an antiphase domain walls on the Cu (001) surface.[15,16]

II. Results and discussion

As the incident HD beam energy varies, certain perpendicular energy conditions are traversed which are at resonance with bound states of rotationally excited molecular HD. The resonance conditions are apparent in specular reflectivity changes. At the specular scattering direction (*i.e.*, the direction in which the $\Delta K = 0$, $\Delta E = 0$, intensity falls) we will find that there are only very rare inelastic scattering events that can contribute significantly to the scattered intensities. Fig. 1 shows an integral specular HD intensity time-of-flight distribution, after transformation to perpendicular incident energies, and with application of a Jacobian factor ($\mathrm{d}E/\mathrm{d}t \propto t^{-3}$). Two distinct types of resonance features are observed; *i.e.*, both maxima and minima. The senses of these features are fully consistent with close-coupling calculations.[17] The specular intensity shows a minimum at resonance if that resonance channel involves an odd numbered rotational state, and a maximum if the resonance rotational quantum number J is even.

By simple subtraction of the HD gas phase rotational energies, from our resonance perpendicular energies, one gets estimates of the $J = 0$ bound state energy levels. (This process is not strictly accurate as the rotational motion is not unperturbed in the bound states.) The estimated $J = 0$ energy levels can then be compared with H_2 and D_2 data in a reduced mass Le Roy plot[11] of the bound state energies. This process both reconfirms the bound state resonance level assignments for H_2 and D_2 isotopes and also defines the HD bound state quantum numbers, ν. The approximate HD energies, incidentally, indicate a physisorption-potential well depth, D, of about 30.5 ± 0.5 meV; this is derived from a third order polynomial fit to the HD Le Roy plot. Incidentally, this HD well is just slightly deeper than that found in a similar experiment for Cu (111) ($D = 27.5$ meV).[8]

The positions and assignments of all observed RMSA resonance energies are presented in Table 1 along with calculation results for the resonances using different potential models. The energies of the bound state resonances were calculated using a numerical, pseudo-spectral wavepacket propagation method that is based on discrete variable and finite basis representations (DVR-FBR).[18] The eigenenergies were determined from the time evolution of an initial wavepacket in the two-dimensional potential by taking the Fourier transform of the wavefunction autocorrelation function. This Fourier transform spectrum is peaked at the eigenenergies and the resolution of the levels is aided by weighting the wavefunction correlation function by a proper window function. The wavepacket was propagated using the standard split operator technique,[19] in which the effect of the potential energy operator and the kinetic energy operator are evaluated in the DVR and FBR, respectively. The FBR in this case consisted of a direct product of plane waves in the z-coordinate and associated Legendre functions in the θ-coordinate. The kinetic energy operator is diagonal in this FBR with rotational energies given by the free

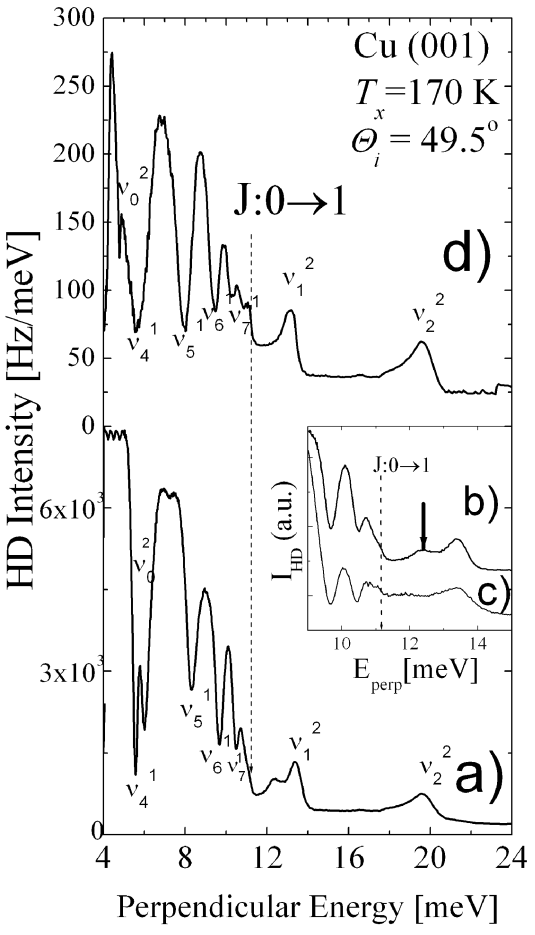

Fig. 1 Specular HD scattering intensities as a function of incident perpendicular energy. The sample position of the sample is fixed such that $\Theta_i = 49.5°$. Resonance minima and maxima are labeled by ν_ν^J, where J is a bound HD rotational quantum number. Curves (a), (b) and (c) are taken for an HD scattering from a clean Cu (001) surface. Curves (b) and (c) show specific details around the 11 meV cutoff in the spectra, measured along two different crystal azimuths: (b) $\Phi = 0°$ and (c) $\Phi = -20°$. Curve (d) shows the HD intensity for scattering from a saturated hydrogen Cu (001) surface. Note: typical intensities decrease by up to 20 times with H adsorption, from (a) to (d).

rotor states. In our calculations we have used gas-phase rotational energies.[20] The DVR consisted of equally sampled points in the z-direction and the Gauss–Legendre quadrature points in the θ-direction.

The "isotropic potential" of Table 1 uses both $V^2(z) = 0$, and $V_{HD}^l(z') = 0$. The latter condition is satisfied by letting α (of eqn. (6)) approach 0. Results of calculations, after the introduction of the $V^2(z)$ term alone (anisotropic potential) are also shown in Table 1, and finally calculation results for the full system with both anisotropic potential and translational–rotational coupling (ATR) are displayed. Both anisotropic and ATR calculations are J and m_J state dependent. The parameterized potentials of Wilzen *et al*[10] are used for the V°(z) and V^2(z) components. The latter $V^2(z)$ form was first deduced from anisotropic calculations and the J (and m_J) splitting of DMSA (aka CMSA) resonances for the H_2 and D_2 systems above the same surface.[11]

Given the sign of the V^2(z) term is negative (just as for the symmetric D_2, H_2 systems,) the preferred molecular orientation is perpendicular to the surface. This is manifest in the lower resonance energies for the $m_J = 0$ states apparent in the anisotropic calculations.

The effects of introducing anisotropy in the potential is clearest in the lowest lying $\nu = 0,1,2$ levels, as the lowest lying levels experience more of the stronger anisotropic interaction potentials. Introduction of the translation to rotation (TR) coupling is also most clearly manifested in the lower levels. The TR destabilizes resonant states with cartwheeling motion, *i.e.*, the TR-coupling slightly counteracts the physisorption anisotropy. In contrast, when the molecule lies down on the surface ($m_J = J$) the resonant levels are least sensitive to the TR coupling. This can be simply understood by considering a molecule with an instantaneously stationary center-of-mass; pure helicoptering motion of this surface molecule does not move the height of the electronic center of molecular hydrogen. Conversely, for cartwheeling motion the potential experienced must oscillate due to simple z motion of the electronic center, and an "average potential" cannot be as low as that at the minimum of the physisorption well.

In the deepest lying levels best agreement, of calculations with experimental data, can be found for the full ATR calculations with the $m_J = 0$ state. This fact is to be expected as the experimental method lends itself only to coupling into the $m_J = 0$ state. The incident beam is exclusively $J = 0$ ($m_J = 0$), momentum transfers are almost exclusively perpendicular to the flat surface, and m_J states are conserved on molecule–surface collision.

Again for the deep lying levels, the deviations between experimental values and calculated values surprisingly are actually worsened by the introduction of the TR coupling. These authors do not believe that TR is absent, but do feel that (an)other systematic contribution(s) to the interaction potentials may be giving rise to the small discrepancy which is most

Table 1 Calculated and experimental bound state resonance energies E_ν for rotationally excited HD above Cu (001)

		Anisotropic potential			Anisotropic potential with TR coupling			Experimental data E_{perp}/meV	
ν, J	Isotropic potential	$m_J = 0$	$m_J = 1$	$m_J = 2$	$m_J = 0$	$m_J = 1$	$m_J = 2$	Cu (001)[a]	Cu (111)[b]
3, 1	2.9	2.3	3.1		2.4	3.1		—	—
4, 1[c]	6.2	5.8	6.3		5.8	6.1		5.9 ± 0.1	6.5
5, 1	8.4	8.1	8.5		8.1	8.4		8.32 ± 0.04	8.7
6, 1	9.7	9.5	9.8		9.5	9.7		9.68 ± 0.01	9.9
7, 1	10.5	10.4	10.5		10.4	10.4		10.48 ± 0.03	10.5
8, 1	10.8	10.8	10.8		10.8	10.8		10.77 ± 0.10	10.9
0, 2	6.6	6.0	6.3	7.4	6.3	6.6	7.4	5.8 ± 0.1	—
1, 2	14.3	13.7	14.0	14.9	13.9	14.2	14.9	13.40 ± 0.05	15.1
2, 2	20.3	19.9	20.1	20.8	20.0	20.2	20.8	19.6 ± 0.1	20.9

[a] Averages of values taken from the observed locations of minima and maxima in 3–5 experiments. [b] Data taken for comparison from ref. 8. [c] Values are uncertain because of overlap of the (0, 2) and (4, 1) states.

Table 2 Experimental bound state resonance conditions and approximate bound states energy levels for HD-H/Cu (001)

Perpendicular energy[a] E_{perp}/meV	Assigned ν J:0 → 1	Assigned ν J:0 → 2	Energy of BSR, E_ν $\Delta J = 1$	$\Delta J = 2$
5.4 ± 0.5	4		−5.66	
7.9 ± 0.2	5		−3.16	
9.4 ± 0.2	6		−1.66	
10.3 ± 0.2	7		−0.76	
10.7 ± 0.2	8		−0.36	
5.0 ± 0.5		0		−28.1
13.0 ± 0.5		1		−20.1
19.6 ± 0.5		2		−13.5

[a] Averages of values taken from the observed locations of minima and maxima.

notable for the J:0 → 2, $\nu = 1$ resonance level. An investigation of one "experimental" possibility follows.

Fig. 1d shows the variation of HD specular intensity with perpendicular energy for scattering from a hydrogen saturated Cu (001) surface. It is clear that with hydrogen saturation, the resonance features are considerably broadened and are shifted to lower perpendicular energies. The maxima or minima positions are listed in Table 2. In this data, the confidence intervals are typically much higher in comparison to the results in Table 1 for the clean Cu (001) surface. The exact resonance points typically are not identical, as H exposures may not be reproduced so exactly. However, using the Le Roy method[11,21] and gas phase rotational energies, a potential well depth of 32.5 meV was found for HD–H/Cu (001); this is only ~1.9 meV deeper than that for the clean copper face.

Any possible H contamination levels on the nominal clean surface are substantially below saturation as He reflectivities are *not* observed to drop measurably, nor show rises as the surface temperature is raised above H_2 desorption temperatures. We will also like to note that the J:0 → 1, ν = 5, 6, 7 resonance positions appear independent of surface temperature. We conclude that small adsorbed hydrogen levels on the "clean" Cu (001) surfaces are *not* sufficient to explain the discrepancies between the ATR $m_J = 0$ calculated values and the experimental values of the lower HD resonant energy levels. One further, and we believe more likely, cause for the slight discrepancies between ATR calculations and experiment is in our assumption of gas phase rotational energies in the bound free-rotor states. For instance, the molecule-surface interaction may cause a slight change of the internuclear distance of the physisorbed molecule resulting in a change of its moment of inertia.

Fig. 1a the maximum at ~12.4 meV (hitherto unassigned as a resonance structure) is assigned to a rare combined rotationally inelastic and diffraction event that is *coincident* with the specular direction. Surface diffraction is comparatively weak, although a noticeable local maximum in the specular intensity is observed when the J:0 → 2 and $G = (+1,0)$ event can contribute to a measured specular intensity. This kinematic coincidence event, which occurs only for a particular incident beam energy ($E_i = 42.6$ meV), is displayed graphically in Fig. 2. In this diagram, $\boldsymbol{k}^{J:0\to2}$ is the outgoing wavevector of an HD molecule that has undergone a J:0 → 2 rotational transition and first order diffraction, and is collinear with all $\boldsymbol{k}_f^{el}$, the outgoing specular elastic wavevectors. The specific $\boldsymbol{k}_f^{el}$ shown for 29.4 meV incident energy, has an E_{perp} of 12.4 meV, and has an identical time-of-flight to the inelastic case shown. The analysis applied to convert flight times to perpendicular scattering energies assumes elastic scattering and gives the false "effective" perpendicular energy, E_{perp}, of 12.4 meV for the rotationally inelastic intensity component, (with $E_i = 42.6$ meV and truly $E_{perp} = 18.0$ meV.

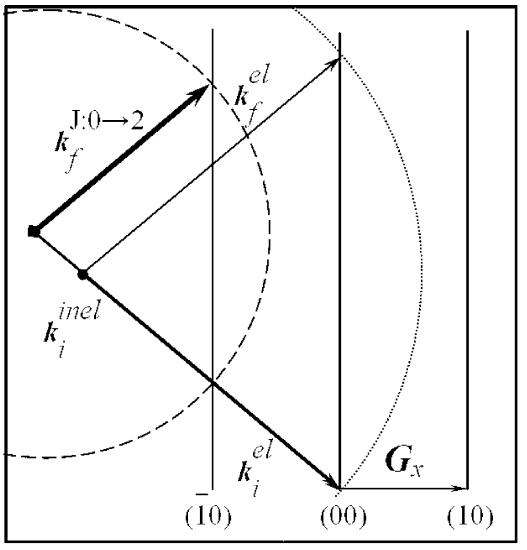

Fig. 2 Vector schematic of the scattering geometry for observation of a coincident first order diffraction and J:0 → 2 rotational transition event. Three vertical lines represent reciprocal lattice rods, $\boldsymbol{k}_i$ and $\boldsymbol{k}_f^{el}$ are the incident- and final elastic-scattering wavevectors, and $\boldsymbol{k}_f^{J:0\to2}$ is an final wavevector that simultaneously satisfies three conditions; (i) a diffraction condition, (ii) is outgoing along a direction that is parallel to $\boldsymbol{k}_f^{el}$, and (iii) obeys energy conservation for the rotational transition. The two circles, centered at the points ● and ■ respectively, are the Ewald sphere projections for J:0 → 0 and J:0 → 2 rotational excitations. For the two illustrated cases, with differing $\boldsymbol{k}_i$, $\boldsymbol{k}_f^{J:0\to2}$ and $\boldsymbol{k}_f^{el}$ are parallel, *i.e.*, both processes can be seen with the same detector geometry, and will exhibit the same total HD flight times to the detector.

Supporting evidence for this coincidence assignment is to be seen in the insert of Fig. 1. The HD perpendicular energy spectra are shown for two scattering azimuths, $\Phi = 0°$ (curve b) and $\Phi = -20°$ (curve c). The absence of the "extra" feature in the $\Phi = -20°$ curve implies loss of a diffraction related condition that can be observed along the high symmetry azimuth. In contrast the RMSA processes remain apparent away from the $\Phi = 0°$ azimuth.

Shorter interval bound state resonance spectra were measured for different substrate temperatures. Selected spectra are presented in Fig. 3, illustrating the temperature dependence of the ν_5^1, ν_6^1 and ν_7^1 resonances for T_x = 133–473 K. The resonance energies do not change noticeably with temperature. However, the FWHM of the observed minima, shown in Fig. 4a, do increase with surface temperature. Surprisingly, the FWHM of all the observed minima are 0.4 meV or higher. A rough extrapolation to $T_x = 0$ K gives a FWHM value of 0.37 ± 0.02 meV. This value is significantly higher than has been observed for Cu (111), and Au (111) (≤0.25 meV),[8] and is also considerably higher than our instrumental resolution (~0.25 ± 0.03 meV). The excesses in minima widths can be interpreted as being in part due to (a) an inhomogeneous broadening, possibly from small hydrogen coverages or small densities of other defects and in part due to (b) a coupling into surface phonons. In addition, the resonance minima (of Fig. 4a, become broader with increasing surface temperature. The effect of this coupling on resonance widths has been studied in the similar case of selective adsorption resonances of H_2 and D_2 molecules on Cu (100).[22] Again this is indicative of the coupling between bound states and surface phonons. As anticipated, the strongest phonon coupling is found for the lower ν resonances. This effect of the greater widths for the deeper bound levels has also been reported[23] for corrugationally mediated selective adsorption resonances in the He–LiF crystal. In the case of the hydrogen covered surface (Fig. 1d), the FWHM of a ν_5^1 level is raised to 0.86 meV and the

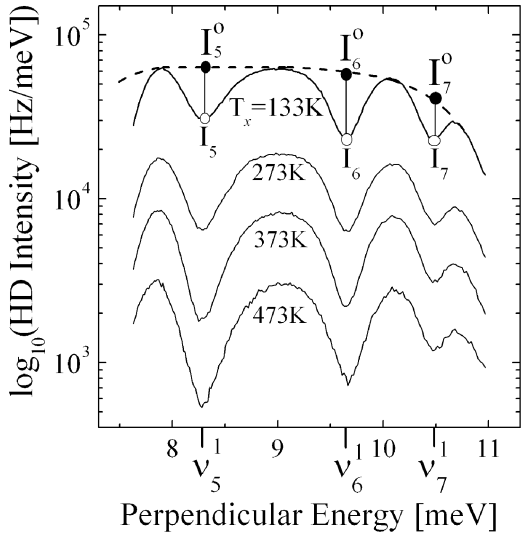

Fig. 3 Measured HD specular peak scattering intensity showing the ν_5^1, ν_6^1, ν_7^1 resonances at several different temperatures on Cu (001). Positions of the energy minima do not change with temperature. Constructed peak intensities, in the absence of resonances, (I_n^0) are shown by a dashed line in the uppermost curve.

FWHM of a ν_6^1 level to 0.53 meV. The enhancement of the H saturated surface line widths we propose must be related to either of the same two causes: (a) further inhomogeneous broadening, from non-uniformity in the adsorbed hydrogen coverage, or from (b) an enhanced homogeneous broadening from an increased surface phonon coupling probability.

Fig. 4b shows explicitly the HD intensity at the resonance minima (I_n) and the extrapolated intensities (I_n^0) (as indicated in Fig. 3). While the Debye–Waller behavior for the I_n^0 intensities can be factored out, the normalized resonance areas (as shown in Fig. 4c, still increase significantly with increasing surface temperatures. Indeed the absolute measured I_n intensities at the resonance conditions decrease faster than the I_n^0 intensities. This observation can be understood in terms of the momentum transfers to the HD molecule that occurs in phonon scattering. *I.e.*, the coupling of the incident HD species to surface phonons (which is apparent in the resonance widths) is also responsible for an increased probability of scattering out of the bound states and into "incoherent or diffuse" directions. The incoherent states may be any of the continuum of free states for $J = 1$ or $J = 0$ rotational levels.

Lastly, the $\nu = 5$ level shows stronger resonance intensity variations in the data of Fig. 4b, than that for the $\nu = 6$ and 7 levels. This is fully consistent with the hypothesis that enhanced phonon scattering probability should exist for in the *lower* lying resonant levels.

In summary, both HD $J = 1$ and $J = 2$ bound state resonances were observed in specular helium reflectivity measurements of the Cu (001) surface. The energy levels were assigned in conjunction with reported H_2 and D_2 resonance levels.[9,10] Small discrepancies in experimentally determined HD resonance levels with calculations (based on the H_2 and D_2 optimized anisotropic interaction potentials[10]) were not improved by consideration of the necessary translational–rotational coupling in the asymmetric HD molecule. Small levels of adsorbed H cannot account for the magnitude of the discrepancies. We believe that, albeit minor, modifications to an optimized interaction potential are *not* required. Instead, we suggest that a more careful consideration of the effects of the interaction potential on rotational energy states would be required for a complete agreement of calculation with experiment.

The lifetime of HD bound states decreases with increasing surface temperature. (An inhomogeneous broadening component in the resonant energy also cannot be discounted.) In addition, the apparent strengths of the HD resonance scattering intensity minima are also influenced by surface temperatures. The Debye–Waller behavior of non-resonant scattered intensities cannot be extrapolated simply to the resonance conditions.

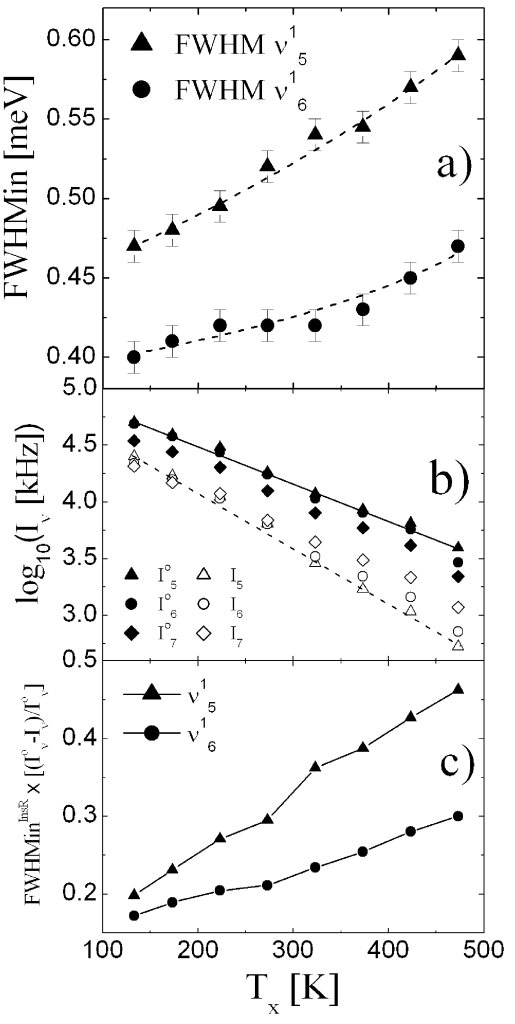

Fig. 4 (a) The measured crystal temperature dependence of HD full (energy) width at half resonance minimum, for ν_5^1, and ν_6^1 resonances. (b) The temperature dependence of specularly scattered HD intensity with (open symbols) and without (solid symbols) resonances, (see Fig. 3). (c) The temperature dependence of a measure of resonant structure strength; an effective resonance area is measured using a $FWHMin^{InsR}$ multiplied by a normalized resonance minimum depth. The full width at half resonance minimum, $FWHMin^{InsR}$, is corrected by the instrumental resolution function, using $FWHMin^{InsR} = (FWHM^2 - (FWHmin^2 - Inst.Resolution^2)^{1/2}$.

Acknowledgements

This work was supported by NSF-CHE 9820661. We would like to thank D. Langreth and K. Burke for informative discussions.

References

1 C.-F. Yu, K. B. Whaley, C. S. Hogg and S. J. Sibener, *J. Chem. Phys.*, 1985, **83**, 4217–4231.
2 S. Andersson and M. Persson, *Phys. Rev. Lett.*, 1993, **70**, 202–205.

3 M. F. Bertino, S. Miret-Artes, J. P. Toennies and G. Benedek, *Surf. Sci.*, 1997, **377–379**, 714–718.
4 R. Berndt, J. P. Toennies and Ch. Wöll, *J. Chem. Phys.*, 1990, **92**, 1468–1477.
5 C.-F. Yu, C. S. Hogg, J. P. Cowin, K. B. Whaley, J. C. Light and S. J. Sibener, *Isr. J. Chem.*, 1982, **22**, 305–314.
6 E. Watts and G. O. Sitz, *J. Chem. Phys.*, 2001, **114**, 4171–4179.
7 M. Balooch, M. J. Cardillo, D. R. Miller and R. E. Stickney, *Surf. Sci.*, 1974, **46**, 358–392.
8 U. Harten, J. P. Toennies and Ch. Wöll, *J. Chem. Phys.*, 1986, **85**, 2249–2258.
9 S. Andersson, L. Wilzen, M. Persson and J. Harris, *Phys. Rev. B*, 1989, **40**, 8146–8168.
10 L. Wilzen, F. Althoff, S. Andersson and M. Persson, *Phys. Rev. B*, 1991, **43**, 7003–7012.
11 S. Andersson, L. Wilzen and M. Persson, *Phys. Rev. B*, 1988, **38**, 2967–2973.
12 K. Svensson, L. Bengtsson, J. Bellman, M. Hassel, M. Persson and S. Andersson, *Phys. Rev. Lett.*, 1999, **83**, 124–127.
13 L. V. Goncharova, J. Braun, A. V. Ermakov, G. G. Bishop, D.-M. Smilgies and B. J. Hinch, *J. Chem. Phys.*, 2001, **115**, 7713–7724.
14 K. B. Whaley, C.-F. Yu, C. S. Hogg, J. C. Light and S. J. Sibener, *J. Chem. Phys.*, 1985, **83**, 4235–4255.
15 A. P. Graham, D. Fang, E. M. McCash and W. Allison, *Phys. Rev. B*, 1998, **57**, 13 158–13 166.
16 I. Chorkendorff and P. B. Rasmussen, *Surf. Sci.*, 1991, **248**, 35–44.
17 R. Schinke, *Surf. Sci.*, 1983, **127**, 283.
18 R. Kosloff, in *Time-Dependent Quantum Molecular Dynamics*, ed. J. Broeckhove and L. Lathouwers, Plenum Press, New York, 1992.
19 M. D. Feit, J. A. Fleck and A. Steigler, *J. Comput. Phys.*, 1982, **47**, 412.
20 K. P. Huber and G. Herzberg, *Molecular Spectra and Molecular Structure*, Van Nostrand Reinhold, New York, 1979.
21 R. J. Le Roy, *Surf. Sci.*, 1976, **59**, 541–553.
22 M. Persson, L. Wilzen and S. Andersson, *Phys. Rev. B*, 1990, **42**, 5331–5334.
23 G. Brusdeylins, R. B. Doak and J. P. Toennies, *J. Chem. Phys.*, 1981, **75**, 1784–1793.